

Counterflow Flame Behavior at Large Lewis Number around Explosive Transition of Deflagration

Akira Tsunoda^{1,2}, Youhi Morii¹, Kaoru Maruta¹

¹Institute of Fluid Science, Tohoku University, Sendai, Miyagi, Japan

¹Graduate School of Engineering, Tohoku University, Sendai, Miyagi, Japan

1 Introduction

Understanding the overall behaviors of deflagration wave under elevated temperature (and pressure) conditions is essential for the development of various applications, including highly efficient internal combustion engines. It has been reported that the flame characteristics of deflagration wave under such environment depend on the significance of chemical reactions in its preheat zone [1], [2]. For instance, low-temperature oxidation in the preheat zone is significant for some specific fuels such as *n*-heptane. The interactions between deflagration and low-temperature oxidation have been studied using stretch-free planar flames [2]–[5], spherical propagating flames [6], [7], and micro flow reactor [8], [9] (see also [10], [11]). Recently, it has been proposed theoretically and numerically [12] that when the unburnt temperature exceeds a certain threshold, no 1D stretch-free planar flame structure exists at Lewis number (Le) is greater than unity because autoignition predominates in the preheat zone of deflagration. This vanishment of 1D stretch-free flame structure is referred to as "Explosive transition of deflagration" [12]. Such behaviors of deflagration wave at $Le > 1$ can be classified into three regions: (I) deflagration with negligible chemical reaction in the preheat zone, (II) deflagration with non-negligible chemical reaction in the preheat zone, and (III) phenomena beyond the explosive transition of deflagration. Fig. 1 depicts the schematics of the behaviors of deflagration wave.

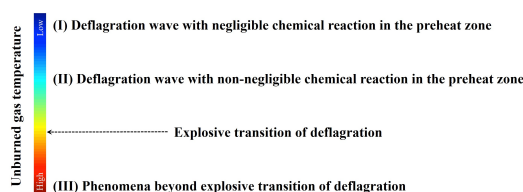


Figure 1: Behaviors of deflagration wave including the explosive transition.

To control the explosive transition, controlling flow residence time in the preheat zone would be crucial. A counterflow flame is advantageous since its flow residence time can be controlled via flame stretch rate [13], [14] while flow residence time of a stretch-free planar flame is uniquely determined as the eigenvalue [15]. In this study, we investigate the relationship between "ignition and deflagration" and the effect of flame stretch on the behaviors of deflagration wave in detail at $Le > 1$ using counterflow flame simulations. Discussion on the explosive transition will be based on findings on the preheat

zone structure influenced by flame stretch and Lewis number [16], [17]. Note that the behaviors of deflagration wave near the explosive transition for stretch-free planar flames with general Lewis numbers is made in this conference [18].

2 The relation between 0D homogeneous ignition and 1D counterflow flame

The detail of the theory discussed here is described in [12]: reaction progress of 0D homogeneous ignition and 1D stretch-free planar flame were compared using a spacio-temporal transformation. A brief description using 0D homogeneous ignition and 1D counterflow flame is given here.

2.1 Governing equations for 0D homogeneous ignition

The governing equations for 0D homogeneous ignition with a multi-step chemical reaction model for the constant pressure and enthalpy case are given by

$$\frac{dY_k}{dt} = \frac{\dot{\omega}_k W_k}{\rho} \quad (k = 1, 2, \dots, K), \quad \frac{dT}{dt} = -\frac{\sum_{k=1}^K \dot{\omega}_k h_k W_k}{\rho c_p}. \quad (1)$$

where t is time, Y_k is the mass fraction of k^{th} species, $\dot{\omega}$ is the chemical production rate of k^{th} species, h_k is the specific enthalpy of k^{th} species, ρ is the mass density, T is the temperature, and K is the total number of chemical species. The Legendre transformation of multivariate function, $f(T, \mathbf{Y}, \rho, t)$ for the normalized Eqs. (1) satisfy $d\tilde{T}/dt = -d\tilde{\Theta}/dt$ relation, where $\tilde{\Theta} = Y_f$ and $\tilde{\Theta} = 1 - C$ for one-step and multi-step chemical reaction models, respectively. C is a progress variable. The normalized temperature and $\tilde{\Theta}$ are defined by $\tilde{T} = (T - T_0)/(T_1 - T_0)$, $\tilde{\Theta} = (\Theta_1 - \Theta)/(\Theta_1 - \Theta_0)$, respectively. $()_0$ and $()_1$ refer to as unburnt and burnt states, respectively. Note that, the Eqs.(1) can be normalized as follows

$$\frac{d\tilde{\Theta}}{dt} = -\frac{\dot{\omega}W}{\rho(\Theta_1 - \Theta_0)}, \quad \frac{d\tilde{T}}{dt} = -\frac{\dot{\omega}hW}{\rho c_p(T_1 - T_0)}. \quad (2)$$

Since the relation between \tilde{T} and $\tilde{\Theta}$ is independent of time, it can be transformed using the residence time τ . It is the total time that the fluid parcel has spent inside a control volume defined by

$$\tau = \int_{x_0}^x \frac{1}{u} dx, \quad (3)$$

where u is the velocity of the fluid parcel and x is the position of the fluid parcel. The total differential of the residence time is $d\tau = u^{-1}dx$. Then Eqs. (2) can be rewritten using the position of fluid parcel using $\tilde{\Theta}$ as follows

$$\rho u \frac{d\tilde{T}}{dx} = -\frac{\dot{\omega}hW}{c_p(T_1 - T_0)}, \quad \rho u \frac{d\tilde{\Theta}}{dx} = -\frac{\dot{\omega}W}{(\Theta_1 - \Theta_0)}. \quad (4)$$

2.2 Governing equations for 1D counterflow premixed flame

The reduced governing equations for 1D counterflow premixed flame along the stagnation-point streamline with a multi-step chemical reaction model are given by

$$\frac{d\rho u}{dx} + 2\rho V = 0, \quad (5)$$

$$\rho u \frac{dV}{dx} + \rho V^2 = -\Lambda + \frac{d}{dx} \left(\mu \frac{dV}{dx} \right), \quad (6)$$

$$\rho c_p u \frac{dT}{dx} = \frac{d}{dx} \left(\lambda \frac{dT}{dx} \right) - \sum_{k=1}^K h_k W_k \dot{\omega}_k, \quad (7)$$

$$\rho u \frac{dY_k}{dx} = -\frac{d}{dx} \left(\rho D_k \frac{dY_k}{dx} \right) + W_k \dot{\omega}_k \quad (k = 1, 2, \dots, K). \quad (8)$$

where u is the axial velocity, v is the radial velocity, $V = v/r$ is the scaled radial velocity, Λ is the pressure eigenvalue independent of x , μ is the dynamic viscosity, λ is the thermal conductivity of the mixture, and D_k is the diffusion coefficient of k^{th} species. The Eqs. (7) and (8) can be rewritten using the normalized temperature and Θ as follows

$$\rho u \frac{d\tilde{T}}{dx} = \frac{1}{c_p} \frac{d}{dx} \left(\lambda \frac{d\tilde{T}}{dx} \right) - \frac{hW\dot{\omega}}{c_p(T_1 - T_0)}, \quad \rho u \frac{d\tilde{\Theta}}{dx} = -\frac{d}{dx} \left(\rho D \frac{d\tilde{\Theta}}{dx} \right) - \frac{W\dot{\omega}}{\Theta_1 - \Theta_0}. \quad (9)$$

The only difference between Eqs. (9) and Eqs. (4) is the first terms on the right-hand sides in Eqs. (9). When the Lewis number of Θ , $Le = \lambda/(\rho c_p D)$ is unity, the mass and energy conservation equations for 0D homogeneous ignition Eqs. (4) after the spacio-temporal transformation using Eq. (3) and for 1D counterflow flame Eqs. (9) using normalized temperature and $\tilde{\Theta}$ are equivalent.

3 Results and discussion

3.1 Numerical methods and conditions

Computations of 0D homogeneous ignition and 1D counterflow flame with a one-step chemical reaction model [19] and a detailed chemical reaction model [20] were performed using Cantera v2.6 [21] with constant pressure and enthalpy. A $C_3H_8/O_2/He$ mixture was used to obtain the mixture of Lewis numbers of both fuel and oxidizer are substantially higher than unity. The ratio of O_2 to He was 21:78 and the equivalence ratio was set to 0.7. Note that a flame should be located far enough from the inlet boundary to minimize the effect of inlet boundary on the temperature and deficient reactant profiles, and to maintain the ideal counterflow velocity field profile.

3.2 1D Counterflow Flame Behavior near the Explosive Transition of Deflagration

To investigate the behavior of deflagration wave near the explosive transition, 0D homogeneous ignition and 1D counterflow flame under elevated temperature conditions after the spacio-temporal transformation were compared. Fig. 2 shows the behavior of 1D counterflow flame and 0D homogeneous ignition under the unburnt temperatures of $T_0 = 500$ K, 1140 K, and 1240 K with the one-step chemical reaction model [19]. Fig. 2a shows the temperature profiles of 0D homogeneous ignition and 1D counterflow

flame after the spacio-temporal transformation using Eq. (3). The 0D homogeneous ignition and 1D counterflow flame reached their maximum gradients at almost the same time under the $T_0 = 1240$ K. Note, the explosive transition of 1D stretch-free planar flame occurred when the 0D homogeneous ignition and 1D stretch-free planar flame reached the maximum temperature gradient at the same order of the residence time [12]. Fig. 2b shows the relationship between the normalized temperature (\tilde{T}) and normalized mass fraction of fuel (\tilde{Y}_f). $\tilde{T} = \tilde{Y}_f$ line is equivalent to the 0D homogeneous ignition and $Le = 1$ condition [12]. All three profiles are convex above $\tilde{T} = \tilde{Y}_f$ line because unburnt fuel was preferentially heated more than it diffuses with $Le > 1$ as in [12], [22]. \tilde{T} at a certain \tilde{Y}_f is larger than $\tilde{T} = \tilde{Y}_f$ line and the reaction progress in $Le > 1$ deflagration proceeds slower than reaction progress lying on $\tilde{T} = \tilde{Y}_f$ line. In other words, there is a possibility that the deflagration at $Le > 1$ may cease to exist when autoignition predominates in the preheat zone. The profile under the $T_0 = 1240$ K in the vicinity of the $(\tilde{T}, \tilde{Y}_f) = (0, 1)$ lies on $\tilde{T} = \tilde{Y}_f$ line. That is, the preheat zone structure of 1D counterflow flame corresponded to the 0D homogeneous ignition.

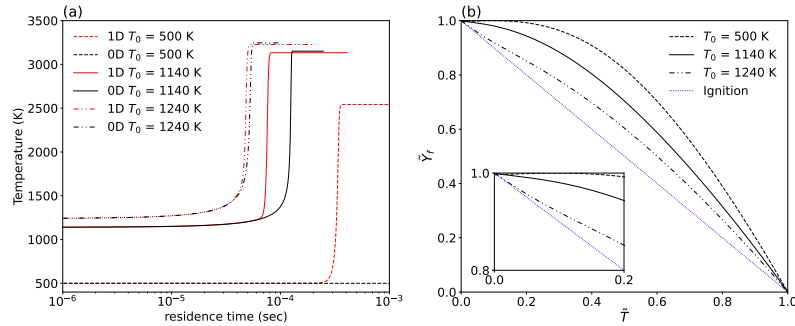


Figure 2: (a) Temperature profiles of 0D homogeneous ignition and 1D counterflow flame after the spacio-temporal transformation. (b) The normalized fuel mass fraction and temperature profiles. The dotted line of $\tilde{T} = \tilde{Y}_f$ is equivalent to the 0D homogeneous ignition and deflagration at $Le = 1$.

Figure 3 shows the behavior of 1D counterflow flame and 0D homogeneous ignition under the inlet temperatures of $T_0 = 800$ K, 1420 K, and 1580 K with the multi-step chemical reaction model [20]. Fig. 3a shows that under $T_0 = 1580$ K, both the 0D homogeneous ignition and 1D counterflow flame had the maximum temperature gradients at nearly the same time, about 300 K higher than that with the one-step chemical reaction model. This should be due to the difference of equilibrium temperatures and of the reaction process, i.e., C_3H_8 does not directly become CO_2 since the multi-step chemical reaction occurred. Fig. 3b shows the relationship between the normalized temperature (\tilde{T}) and the normalized progress variable ($1 - \tilde{C}$). The progress variable was defined as $C = Y_{CO} + Y_{CO_2} + Y_{H_2} + Y_{H_2O}$ [23] which allowed the simulation to accurately reproduce the phenomena was employed here. Since the fuel was depleted before the temperature reached the final state, \tilde{Y}_f and \tilde{T} have lost one-to-one correspondence (bijection). Therefore, the relationship between \tilde{T} and \tilde{Y}_f no longer represents the characteristics of overall reaction progress. For the sake of comparison with Fig. 2, the relation of $(1 - \tilde{C})$ and \tilde{T} is shown. All three profiles are convex above the $\tilde{T} = 1 - \tilde{C}$ line as in these with the one-step reaction model. The profile under the $T_0 = 1580$ K in the vicinity of the $(\tilde{T}, 1 - \tilde{C}) = (0, 1)$ lies on the $\tilde{T} = 1 - \tilde{C}$ line. That is, the preheat zone of 1D counterflow flame corresponded to the 0D homogeneous ignition if the appropriate \tilde{C} was used as $\tilde{\Theta} = 1 - \tilde{C}$.

4 Conclusions

The relationship between "ignition and deflagration" and the effect of flame stretch on the behavior of deflagration wave near the explosive transition of deflagration were investigated at $Le > 1$. The 0D ho-

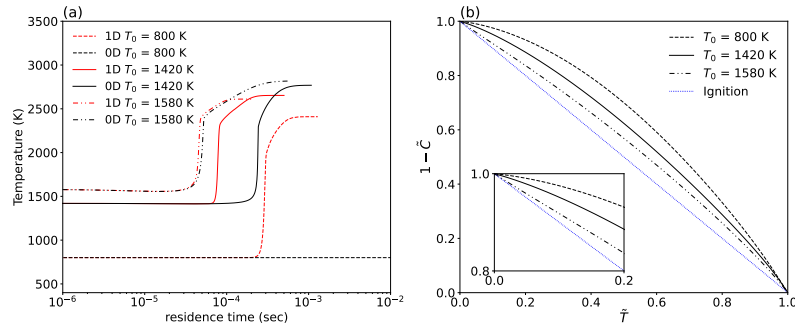


Figure 3: (a) Temperature profiles of 0D homogeneous ignition and 1D counterflow flame after the spacio-temporal transformation. (b) The normalized progress variable and temperature profiles. The dotted line of $\tilde{T} = 1 - \tilde{C}$ is equivalent to the 0D homogeneous ignition and deflagration at $Le = 1$.

mogeneous ignition and 1D counterflow flame reached their maximum temperature gradients at almost the same time under the $T_0 = 1240$ K with the one-step chemical reaction model and the $T_0 = 1580$ K with the multi-step chemical reaction model, while the explosive transition of 1D stretch-free planar flame occurred when the 0D homogeneous ignition and 1D stretch-free planar flame reached the maximum temperature gradients at the same order of the residence time [12]. It was suggested that the flame stretch would suppress the explosive transition. This can qualitatively explain the effect of turbulence on the knocking onset reported in the literature [24]. Under such conditions, the profile in the vicinity of $(\tilde{T}, \tilde{Y}_f) = (1, 0)$ lied on $\tilde{Y}_f = \tilde{T}$ line in $\tilde{T} - \tilde{Y}_f$ plane with one-step chemical reaction model. This indicated that the preheat zone of 1D counterflow flame is being equivalent to 0D homogeneous ignition. These deflagrations can be classified in the type (II) near the explosive transition. The equivalent phenomena could be confirmed with multi-step chemical reaction model if the progress variable \tilde{C} is used instead of \tilde{Y}_f .

Acknowledgement

This work was partially supported by JSPS KAKENHI Grant Number 19KK0097.

References

- [1] R. Sankaran, "Propagation velocity of a deflagration front in a preheated autoigniting mixture," in *9th US Combustion Meeting*, Cincinnati, Ohio, 2015.
- [2] A. Krisman, E. R. Hawkes, and J. H. Chen, "The structure and propagation of laminar flames under autoignitive conditions," *Combustion and Flame*, vol. 188, pp. 399–411, 2018.
- [3] T. Zhang and Y. Ju, "Structures and propagation speeds of autoignition-assisted premixed n-heptane/air cool and warm flames at elevated temperatures and pressures," *Combustion and Flame*, vol. 211, pp. 8–17, 2020.
- [4] A. Ansari, J. Jayachandran, and F. N. Egolfopoulos, "Parameters influencing the burning rate of laminar flames propagating into a reacting mixture," *Proc. Comb. Inst.*, vol. 37, no. 2, pp. 1513–1520, 2019.
- [5] X. Gong and Z. Ren, "Flame speed scaling in autoignition-assisted freely propagating n-heptane/air flames," *Proc. Comb. Inst.*, vol. 38, no. 2, pp. 2153–2161, 2021.

- [6] T. Zhang, A. J. Susa, R. K. Hanson, and Y. Ju, "Studies of the dynamics of autoignition assisted outwardly propagating spherical cool and double flames under shock-tube conditions," *Proc. Comb. Inst.*, vol. 38, no. 2, pp. 2275–2283, 2021.
- [7] Q. Yang and P. Zhao, "Minimum ignition energy and propagation dynamics of laminar premixed cool flames," *Proc. Comb. Inst.*, vol. 38, no. 2, pp. 2315–2322, 2021.
- [8] K. Maruta, T. Kataoka, N. Kim, S. Minaev, and R. Fursenko, "Characteristics of combustion in a narrow channel with a temperature gradient," *Proc. Comb. Inst.*, vol. 30, no. 2, pp. 2429–2436, 2005.
- [9] K. Akita, Y. Morii, Y. Murakami, H. Nakamura, T. Tezuka, and K. Maruta, "Dynamics of FREI with/without cool flame interaction," *Proc. Comb. Inst.*, 2022.
- [10] Y. Ju, C. B. Reuter, O. R. Yehia, T. I. Farouk, and S. H. Won, "Dynamics of cool flames," *Progress in Energy and Combustion Science*, vol. 75, p. 100787, 2019.
- [11] Y. Ju, "Understanding cool flames and warm flames," *Proc. Comb. Inst.*, vol. 38, no. 1, pp. 83–119, 2021.
- [12] Y. Morii and K. Maruta, "What connects ignition and deflagration? – on explosive transition of deflagration," *arXiv*, 2022. DOI: 10.48550/arxiv.2212.01978.
- [13] M. Vera and A. Liñán, "Large activation energy analysis of nonadiabatic strained premixed laminar flames with nonunity lewis numbers," *Combustion Science and Technology*, pp. 1–46, 2022.
- [14] P. A. Libby, A. Liñán, and F. A. Williams, "Strained premixed laminar flames with nonunity lewis numbers," *Combustion Science and Technology*, vol. 34, no. 1, pp. 257–293, 1983.
- [15] F. A. Williams, *Combustion Theory*. Persure books publishing, 1985.
- [16] J. H. Ferziger and T. Echehki, "A simplified reaction rate model and its application to the analysis of premixed flames," *Combustion Science and Technology*, vol. 89, no. 5, pp. 293–315, 1993.
- [17] A. Tsunoda, T. Akiba, H. Nakamura, Y. Morii, T. Tezuka, and K. Maruta, "Computational study on lean and rich combustion of flame ball, counterflow flame and planar flame: Their limits and stoichiometries," *Proc. Comb. Inst.*, DOI: 10.1016/j.proci.2022.07.158.
- [18] Y. Morii, A. Tsunoda, and K. Maruta, "Lewis number effect on explosive transition of stretch-free flamt flame," in *29th International Colloquium on the Dynamics of Explosions and Reactive Systems*, 2023.
- [19] Cerfacs, *1 global step mechanism for propane*. [Online]. Available: https://www.cerfacs.fr/cantera/docs/mechanisms/propane-air/1S_C3H8_CM1.
- [20] Mechanical and U. o. C. AerospaceEngineering, *The san diego mechanism*, 2016. [Online]. Available: <http://web.eng.ucsd.edu/mae/groups/combustion/index.html>.
- [21] G. David G., S. Raymond L., M. Harry K., and W. Bryan W., *Cantera: An object-oriented software toolkit for chemical kinetics, thermodynamics, and transport processes*, 2021. DOI: 10.5281/zenodo.4527812.
- [22] A. J. Aspden, M. S. Day, and J. B. Bell, "Lewis number effects in distributed flames," *Proc. Comb. Inst.*, vol. 33, no. 1, pp. 1473–1480, 2011.
- [23] M. Ihme and H. Pitsch, "Prediction of extinction and reignition in nonpremixed turbulent flames using a flamelet/progress variable model: 2. application in LES of sandia flames d and e," *Combustion and Flame*, vol. 155, no. 1, pp. 90–107, 2008.
- [24] M. B. Luong, S. Desai, F. E. H. Pérez, R. Sankaran, B. Johansson, and H. G. Im, "A statistical analysis of developing knock intensity in a mixture with temperature inhomogeneities," *Proc. Comb. Inst.*, vol. 38, pp. 5781–5789, 2021.